Biosensors and Bioelectronics 80 (2016) 654–660

Contents lists available at ScienceDirect

Biosensors and Bioelectronics

journal homepage: www.elsevier.com/locate/bios

Accurate and easy-to-use assessment of contiguous DNA methylation sites based on proportion competitive quantitative-PCR and lateral flow nucleic acid biosensor

Wentao Xu [a,c,1], Nan Cheng [a,1], Kunlun Huang [a,c], Yuehe Lin [b], Chenguang Wang [a], Yuancong Xu [a], Longjiao Zhu [a], Dan Du [b], Yunbo Luo [a,*]

[a] Beijing Advanced Innovation Center for Food Nutrition and Human Health, College of Food Science & Nutritional Engineering, China Agricultural University, Beijing 100083, China
[b] School of Mechanical and Materials Engineering, Washington State University, Pullman 99164, USA
[c] Beijing Laboratory for Food Quality and Safety, College of Food Science and Nutritional Engineering, China Agricultural University, Beijing 100083, China

ARTICLE INFO

Article history:
Received 25 November 2015
Received in revised form
13 February 2016
Accepted 15 February 2016
Available online 16 February 2016

Keywords:
DNA methylation
Proportion competitive quantitative PCR
Lateral flow nucleic acid biosensor

ABSTRACT

Many types of diagnostic technologies have been reported for DNA methylation, but they require a standard curve for quantification or only show moderate accuracy. Moreover, most technologies have difficulty providing information on the level of methylation at specific contiguous multi-sites, not to mention easy-to-use detection to eliminate labor-intensive procedures. We have addressed these limitations and report here a cascade strategy that combines proportion competitive quantitative PCR (PCQ-PCR) and lateral flow nucleic acid biosensor (LFNAB), resulting in accurate and easy-to-use assessment. The *P16* gene with specific multi-methylated sites, a well-studied tumor suppressor gene, was used as the target DNA sequence model. First, PCQ-PCR provided amplification products with an accurate proportion of multi-methylated sites following the principle of proportionality, and double-labeled duplex DNA was synthesized. Then, a LFNAB strategy was further employed for amplified signal detection via immune affinity recognition, and the exact level of site-specific methylation could be determined by the relative intensity of the test line and internal reference line. This combination resulted in all recoveries being greater than 94%, which are pretty satisfactory recoveries in DNA methylation assessment. Moreover, the developed cascades show significantly high usability as a simple, sensitive, and low-cost tool. Therefore, as a universal platform for sensing systems for the detection of contiguous multi-sites of DNA methylation without external standards and expensive instrumentation, this PCQ-PCR-LFNAB cascade method shows great promise for the point-of-care diagnosis of cancer risk and therapeutics.

1. Introduction

The assessment of DNA methylation level is of particular importance because DNA methylation is not only a major form of epigenetic information in mammalian cells but also a highly specific biomarker for some cancers and aging (Razin and Riggs, 1980; Tsou et al., 2002; Chodavarapu et al., 2010). In particular, the detection of the proportion of site-specific DNA methylation can be used to determine specific tissues and diseases (Porter et al., 2007; Wang et al., 2010; Suzuki et al., 2006). The development of sensitive DNA methylation level detection platforms using fundamental life science research and early cancer diagnosis has received great attention in recent years. Various PCR-based strategies demonstrated unique advantages such as high sensitivity and rapid analysis with spatial resolution (Erlich et al., 1991; Bartlett and Stirling, 2003; Watson, 2012) have been developed for examination of DNA methylation levels, including accurate examination methods, such as restriction enzyme-PCR (Hughes and Jones, 2007), methylation-specific PCR (Herman et al., 1996), methyLight (Ogino et al., 2006), pyrosequencing and digital PCR (Tost and Gut, 2007; Shelton et al., 2014), and rapid detection techniques, such as loop-mediated isothermal amplification (LAMP), and hybridization chain reaction circle amplification (HCR) (Zerilli et al., 2010; Bi et al., 2013). However, accurate determination methods require a standard curve and present differences between each tube reaction in most cases, while rapid detection

* Correspondence to: Laboratory of Food Safety and Molecular Biology, College of Food Science and Nutritional Engineering, China Agricultural University, No. 17 Qinghua East Road, Haidian District, Beijing 100083, China.
Tel./fax: +86 10 62738793.
E-mail address: lyb@cau.edu.cn (Y. Luo).
[1] These authors contributed equally to this work and should be considered co-first authors.

http://dx.doi.org/10.1016/j.bios.2016.02.039
0956-5663/

techniques exhibit only moderate accuracy and high contamination risk; all the above methods have difficulty in providing information on the level of methylation at specific contiguous multi-sites. Moreover, traditional PCR product detection technologies require labor-intensive procedures, harsh experimental conditions, and high experimental cost to obtain data, dramatically hampering their implementation for wider and more versatile applications. Therefore, a novel PCR-based technique design as an ideal tool for accurate, independence of stand curve, easy-to-use, cost-effective and field-applicable detection of contiguous multi-sites of DNA methylation is highly desirable.

Two different strategies have been widely employed to achieve the accurate quantitative detection of PCR products: real-time quantitative PCR and competitive quantitative PCR. In the first case, expensive equipment and a fluorescent chemical reagent challenge promotion, and starting point quantitative technology is not suitable for in situ detection; thus, it is not a reasonable solution (Nolan and Bergkvist, 2013). In the second case, the concept of an exogenous reference gene was introduced to achieve an accurate end-point quantitative result without a standard curve; instead, it measures the target sites and internal reference site within the same tube, which was quantified simply and conveniently by proportion (Zachar et al., 1993; Zhou et al., 2015). Here, we propose the proportion competitive quantitative PCR (PCQ-PCR) by virtue of an internal reference gene for multi-methylated site detection to achieve a novel sensing platform with a predictably satisfactory accuracy and easy operation. To obtain easy-to-use assessment of PCR products, the lateral flow nucleic acid biosensor (LFNAB), as a new alternative technology, has attracted significant attention in recent years due to being affordable, user-friendly, rapid and robust (Liana et al., 2012; Parolo and Merkoçi, 2013; Ge et al., 2014). The LFNABs were usually designed for testing a wide variety of analytes, including genetically modified organisms (Mao et al., 2009); pathogenic organisms, such as *Escherichia coli* (Noguera et al., 2011) and *Salmonella* (Fang et al., 2014); viruses, such as *influenza A virus* (Kim et al., 2014) and *Novel Avian-Origin Influenza A* (Ge et al., 2013); heavy metals, such as copper (Fang et al., 2010); health states, such as tuberculosis (Torres-Chavolla and Alocilja, 2011) and human African trypanosomiasis (Njiru, 2011); or biomarkers of diseases, such as microRNA (Gao et al., 2014) and gene mutation (He et al., 2012). However, there has been not any report on DNA methylation analysis using LFNAB, neither single-site nor multi-sites assessment. Moreover, to the best of our knowledge, no research efforts have yet found a way to combine these strategies into one system, especially in the case of the production of PCQ-PCR that is extremely suitable for LFNAB to amplify the signal and obtain accurately proportioned results.

In this study, we employed a cascade strategy combining PCQ-PCR with LFNAB to develop a PCQ-PCR-LFNAB cascade system for amplifying the sensing of contiguous multi-sites of DNA methylation with accuracy and usability. The $P16^{INK4a}$ (*p16*) tumor suppressor gene, also known as CDKN2A, MTS1, INK4a and CDK4I, was chosen as the model and can show aberrant promoter region methylation in many tumor types (Nakayama et al., 2011; Jha et al., 2012). Moreover, a significantly higher proportion of hypermethylated *p16* has been identified at advanced clinical stages (Gu et al., 2013; Wang et al., 2014). As a model, the biosensor was applied for the assessment of three contiguous methylated sites (defined as “a”, “b” and “c”) and an internal reference site (defined as “ir”) of the *p16* gene. The attractive characterostics of the PCQ-PCR-LFNAB cascade were reported in the following sections.

2. Materials and methods

2.1. Materials

Chloroauric acid tetrahydrate ($HAuCl_4 \cdot 4H_2O$), sucrose, hydroxylamine, NaCl, $Na_3PO_4 \cdot 12H_2O$, Tween 20, Triton X-100, trisodium citrate, sodium citrate dihydrate, bovine serum albumin (BSA), sodium chloride–sodium citrate (SSC) buffer 20 concentrate (pH 7.0), phosphate buffered saline (PBS, pH 7.4, 0.01 M), and borate buffer (BB, pH 9.0, 0.1 M) were purchased from Sigma Chemical Company (St. Louis, MO, USA). The PCR buffer, rTaq DNA polymerase and deoxynucleotide solution mixture (dNTPs) were from TaKaRa Biotech (Dalian, China). Biotin-dUTP was obtained from Tiandz Gene Technology Co., Ltd. (Beijing, China). Bst DNA polymerase was from New England Biolabs (Beijing, China). The QIAamp DNA blood mini kit was purchased from Qiagen (Hilden, Germany). The anti-biotin antibody, anti-rhodamine antibody, anti-digoxin antibody, anti-FITC antibody, anti-hex antibody and goat anti-mouse IgG were purchased from Abcam Inc. (Cambridge, MA, USA). Backing cards (HF000MC100), glass fiber sample pads (CFSP001700), conjugation pad (GFCP000800), nitrocellulose membranes (135 s) and absorbent pads (CFSP001700) were purchased from Millipore (Bedford, MA, USA). Another type of nitrocellulose membrane (CN140) was purchased from Sartorius (Göttingen, Germany).

The sequences of oligonucleotides, including target template DNAs [M0; M1 ($M1^a$, $M1^b$, and $M1^c$); M2 ($M2^{ab}$, $M2^{ac}$, and $M2^{bc}$) and M3 ($M3^{abc}$)], ddNTP-modified stem-loop primers (a, b, c, and ir), universal forward (F) and specific reverse primers (Rhodamine-R^a, Digoxin-R^b, FITC-R^c and Hex-R^{ir}), that were used in this work were synthesized by TaKaRa Biotech (Dalian, China) and are presented in Table S1. Synthetic oligonucleotides M1 ($M1^a$, $M1^b$, and $M1^c$), M2 ($M2^{ab}$, $M2^{ac}$, and $M2^{bc}$) and M3 ($M3^{abc}$), as the methylated target template DNAs, and M0, as the unmethylated target template DNA, were used in this study.

2.2. PCQ-PCR procedure

The three methylated sites (a, b and c) and a universal site (ir) of the *p16* gene were amplified by PCQ-PCR based on a previous study with slight modifications (Chen et al., 2005). Briefly, the detection was performed in a 50 μL reaction containing 1 × PCR Buffer; 0.2 mM dATP, dGTP, and dCTP; 0.1 mM dTTP; 0.1 mM biotin-dUTP; 0.4 μM each stem-loop primer (a, b, c, and ir); 0.8 μM universal forward primer (F); 0.4 μM each specific reverse primer (Rhodamine-R^a, Digoxin-R^b, FITC-R^c and Hex-R^{ir}); 4 U of Bst DNA polymerase; 2.5 U of rTaq DNA polymerase; and 1 μL of target. First, the reactions were incubated in a Bio-Rad PCR thermal cycler (California, USA) for 30 min at 16 °C, 30 min at 42 °C and 5 min at 95 °C. Then, the reactions went into the PCR cycle for 30 s at 95 °C, 30 s at 60 °C and 30 s at 72 °C in 35 cycles. Finally, the reactions were held at 72 °C for 10 min and stored at 4 °C for further research. The resulting PCQ-PCR products should contain rhodamine (digoxin, FITC, or hex) at the end and biotin in the middle.

2.3. LFNAB procedure

The LFNAB consisted of the following five components: sample pad, conjugate pad, nitrocellulose membrane, absorbent pad, and backing. The sample pad was made from glass fiber and saturated with a buffer (pH 8.0) containing 0.25% Triton X-100, 0.1 M BB, and 0.15 M NaCl. Then, the pad was dried at 37 °C for 2 h and stored in a desiccator at room temperature. For the differentiation of the a-, b- and c-methylated sites, three test lines (TL1, TL2, and TL3) were prepared by dispensing anti-rhodamine antibody (1.0 mg/mL), anti-digoxin antibody (1.0 mg/mL) and anti-FITC antibody

(1.0 mg/mL) solutions at different locations on the nitrocellulose membrane using BioDot BioJet BJQ 3000 dispenser (Irvine, CA). In order to ensure the proper function of the PCQ-PCR and LFNAB, an internal reference line (IRL) and a control line (CL) were added by spraying anti-hex antibody (1.0 mg mL^{-1}) and goat anti-mouse IgG (1.0 mg mL^{-1}) solutions, respectively. The distance between each line was approximately 4 mm. The nitrocellulose membranes were then dried overnight at 37 °C and stored at 4 °C in a dry state until use. The different pads were assembled on a plastic adhesive backing card with an overlap between them of approximately 1–2 mm in order to ensure that the solution could migrate through the strip. Strips were cut at a width of 3 mm using a Bio-Dot Paper Cutter module CM4000 (Irvine, CA). Finally, the anti-biotin-Au-NPs conjugates, whose functionalization process is described in the Supporting information, were dropped on the conjugate pad using Bio-Dot AirJet AJQ 3000 dispenser (Irvine, CA), used immediately, or sealed and stored under dry conditions at room temperature until use.

2.4. PCQ-PCR-LFNAB cascade procedure

Following PCQ-PCR, 50 µL of running buffer (4 × SSC, 2% BSA, and 0.05% Tween-20, pH 7.0) was mixed with 50 µL of the amplification product solution; then, the mixture was applied to the sample pad of the LFNAB and migrated up by capillary force. The lines were evaluated visually within 5 min. The naked-eye detection of DNA methylation was performed simply by observing the relative intensity of TLs and IRL of each single LFNAB, which differed between methylated and unmethylated samples. For quantitative measurements, the LFNAB was inserted into the portable "strip reader" instrument DT2050 purchased from Shanghai Goldbio Tech. Co., Ltd. (Shanghai, China), and the optical intensities of the red lines were recorded with "Goldbio strip reader" software, which could determine parameters, such as peak height and area integral. Each sample was detected 3 times, and the average value of three measurements was used.

3. Results and discussion

3.1. Design of the PCQ-PCR-LFNAB cascade sensing system

The design of this novel cascade is shown in Scheme 1. PCQ-PCR is used to generate numerous of biotin- and rhodamine (digoxin, FITC, and hex)-attached duplex DNAs. In a typical assay, in the presence of target with three methylated sites ($M3^{abc}$), the four competitive stem-loop primers recognize and hybridize with complementary a, b, c and ir sites, respectively (step 01). The specific stem-tail at the 3′-end of stem-loop primer thus anneals with the stem and triggers a polymerization reaction in the presence of dNTP solution mixed with biotin-dUTP and Bst DNA polymerase (step 02). Next in the process of denaturation, the stem-loop primer then undergoes a conformational change, leading to stem separation (step 03). Finally, the universal forward primer and the rhodamine (digoxin, FITC, or hex)-modified reverse specific primer in excess were used to complete the PCR process in the presence of rTaq DNA polymerase and dNTP solution mixed with biotin-dUTP, after which a complementary DNA is synthesized, forming a biotin- and rhodamine (digoxin, FITC, or hex)-attached duplex DNA (step 04). The accuracy of the PCQ-PCR procedure was based on the approximately equal amplification efficiencies of the primers, as demonstrated by real-time PCR experiments in Fig. S1. Throughout this cyclical process, numerous biotin- and rhodamine (digoxin, FITC, or hex)-attached duplex DNA complexes are produced.

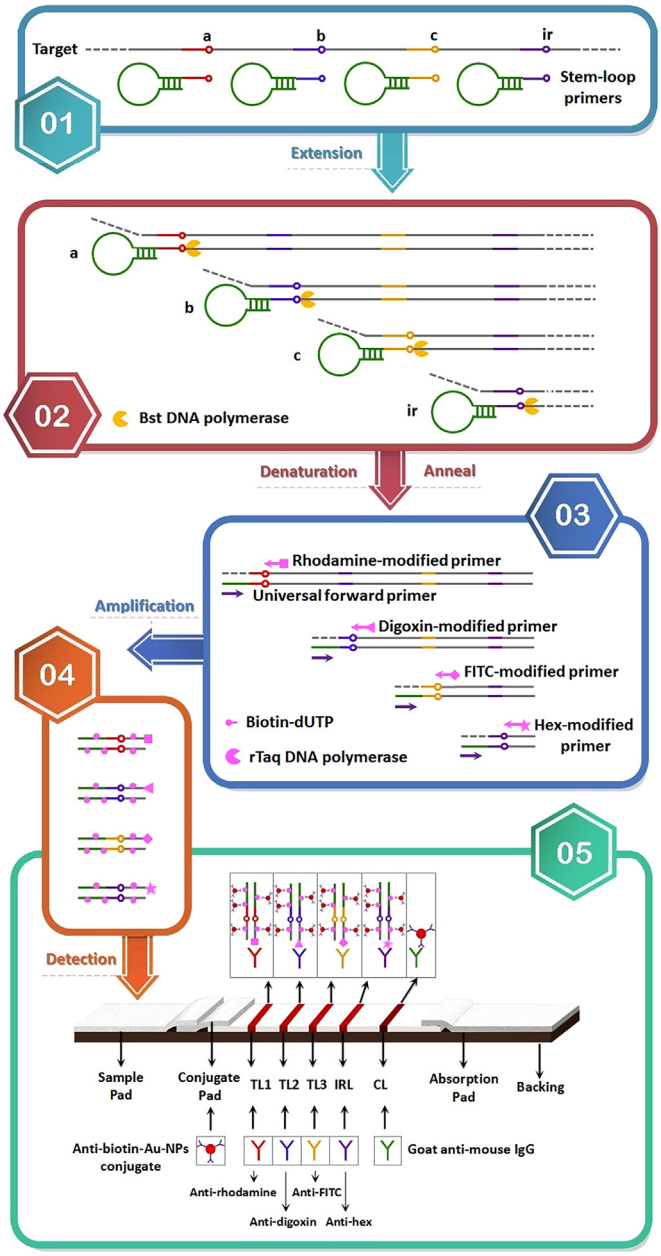

Scheme 1. Schematic illustration of the design of the PCQ-PCR-LFNAB cascade sensing system.

The easy-to-use detection of the amplified duplex DNA complexes, by using the LFNAB, is illustrated in step 05. The principle of the LFNAB measurement is based on the sandwich type of "(anti-biotin-Au-NPs)-(target DNA complexes)-(relevant antibody)" hybridization reactions. The sample solution containing the desired amount of target DNA products with three methylated sites ($M3^{abc}$) and running buffer was applied to the sample pad. Subsequently, the solution migrated by capillary action and passed the conjugate pad, anti-biotin-Au-NPs conjugates were rehydrated, hybridization between the target DNA and anti-biotin-Au-NPs conjugates occurred, and the formed (anti-biotin-Au-NPs)-(target DNA) complexes continued to migrate along the strip. When the resulting complexes reached TLs and IRL, they were captured by the second hybridization between the target DNA and anti-rhodamine antibody, anti-digoxin antibody, anti-FITC antibody, and anti-hex antibody, respectively. The four characteristic red bands could be observed because of the accumulation of Au-

NPs when migrating along the LFNAB. Then, the excess anti-biotin-Au-NPs conjugates continued to migrate through CL and were captured by a secondary antibody, thus forming another red band. The red band on IRL indicated that the PCQ-PCR amplification worked properly, and the red band on CL indicated that the biosensor worked properly.

Typical picture of LFNABs in the present of other variety targets was presented in Fig. S2. Red band on any of TLs indicated a "methylated-site" result, while no red band indicated an "unmethylated-site" result. A qualitative analysis was simply performed by observing the color change of TLs, and the quantitative measurements were accurate by using self-contained quantitative system of the biosensor instead of a traditional standard curve quantitative system to avoid individual differences. The relative intensity is defined as the peak area of TL divided by the peak area of the IRL of each individual biosensor. Therefore, the different relative intensity reflected the various exact level of DNA methylation at different sites (see details in Fig. S3), indicating that PCQ-PCR-LFNAB cascade sensing system can detect DNA multi-methylation.

3.2. Optimization of the LFNAB

To improve sensitivity of the LFNAB, various preparation and detection parameters were systematically investigated by comparing the analytical performances of the LFNAB, including membrane materials, the concentration of the anti-biotin antibody for preparing anti-biotin-AuNP conjugates, the amount of anti-biotin-AuNP conjugates dispensed on the conjugate pad, the concentration of antibody dispensed on the lines, reaction time, and running buffers (see detail discussion in Supporting information). As shown in Fig. 1A, the better performance of LFNAB was obtained with Millipore 135 s nitrocellulose membrane. The concentration of 1 μg mL^{-1} anti-biotin antibody was the best option to prepare the anti-biotin-Au-NP conjugates (Fig. 1B). And 1.5 μL of anti-biotin-AuNP conjugates on the conjugate pad was used as the optimal volume (Fig. 1C). Besides, 1.0 mg mL^{-1} anti-rhodamine antibody, 1.0 mg mL^{-1} anti-digoxin antibody, 1.0 mg mL^{-1} anti-FITC antibody, and 1.0 mg mL^{-1} anti-hex antibody were used to prepare the lines (Fig. 1C). The best reaction time of LFNAB was greater than 3 min (Fig. 1D). In Fig. 1E, the 4 × SSC+2% BSA+0.05% Tween-20 buffer provided the optimum combination for clear bands, rapid tests, and background elimination was choosed as porper running buffer to detect the PCQ-PCR products on the LFNAB.

3.3. Analytical performances

Under optimal experimental conditions, we evaluated the analytical performance of the PCQ-PCR and LFNAB analytical procedure in the following aspects:

(1) Specificity and sensitivity: because practical samples are always a mixture of different concentrations of methylated and unmethylated DNA sites, we tried to detect the mixture of M3 and M0 target DNA. Fig. 2 displays the typical photo image of the LFNAB with the current increase percentage of the M3/(M3+M0) mixture at ratios of 0%, 5%, 25%, 40% and 100%. The sensitivity of LFNAB was set as the minimal ratios of PCQ-PCR products that resulted in specific lines on TLs. In contrast, the unmethylated DNA did not produce a detectable signal, indicating the excellent detection specificity of this method for methylated DNA. For visual qualitative detection, the red band in the TLs could be detected at levels as low as 5% of M3. The intensity of the test band increased with the increasing of M3 DNA proportions up to 100%. The unmethylated DNA did not produce a detectable signal indicating the excellent detection specificity of this method for methylated DNA.

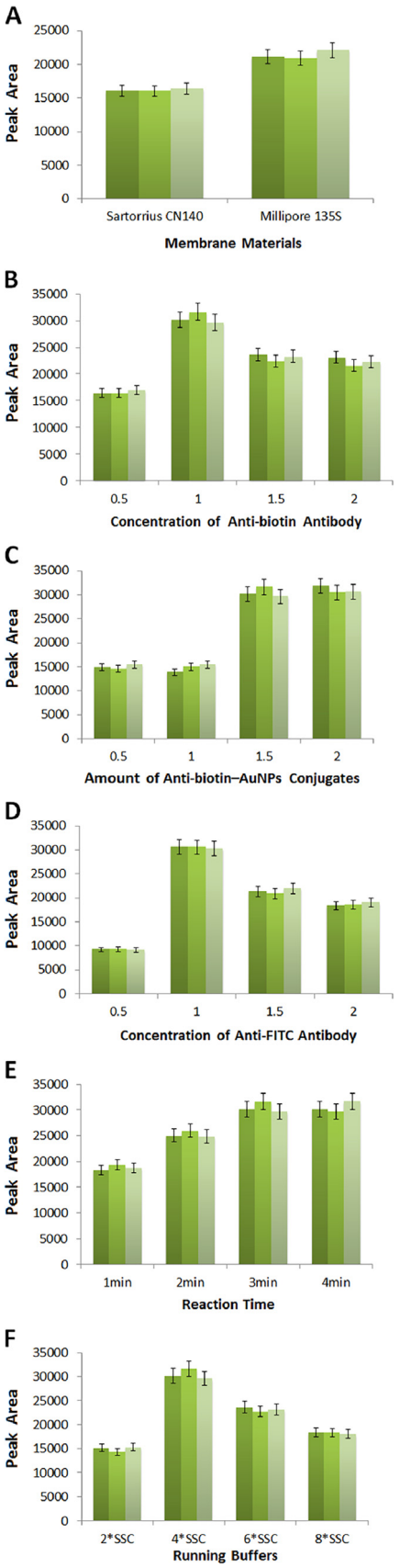

Fig. 1. (A) Effect of membrane materials on the peak area of LFNAB; (B) Effect of the concentrations of anti-biotin antibody on the peak area of LFNAB; (C) Effect of the amount of anti-biotin-AuNPs conjugates on the peak area of LFNAB; (D) Effect of the concentrations of antibody on the lines on the peak area of LFNAB; (E) Effect of the reaction time on the peak area of LFNAB; and (F) Effect of the running buffers on the peak area of LFNAB.

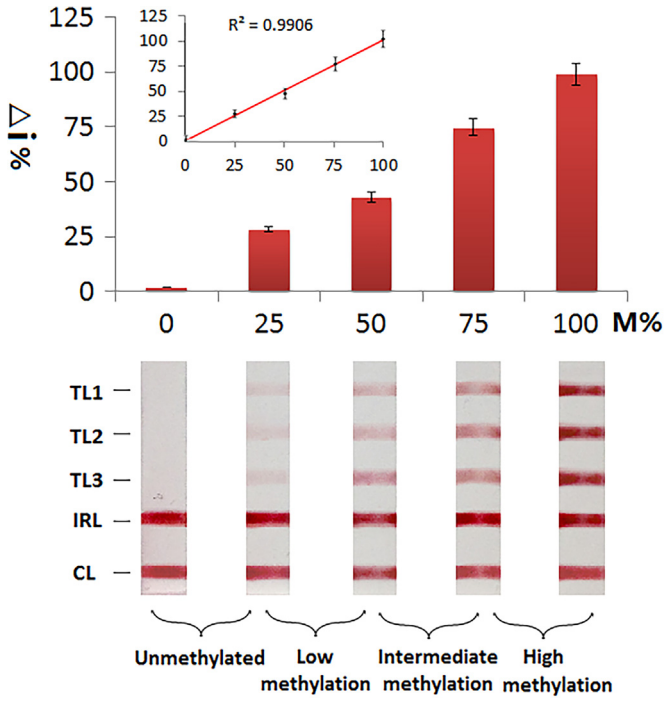

Fig. 2. Typical photograph images (bottom) and corresponding intensities (top) of the LFNABs in the presence of different concentrations of M3 in the mixture between M3 and M0. The intensities of the bands were recorded by strip reader. M% is the percentage of M3 present in all samples: M%=M3/[M3+M0]. For left to right, the ratios of M% are 0, 5%, 25%, 40% and 100%. (For interpretation of the references to color in this figure, the reader is referred to the web version of this article.)

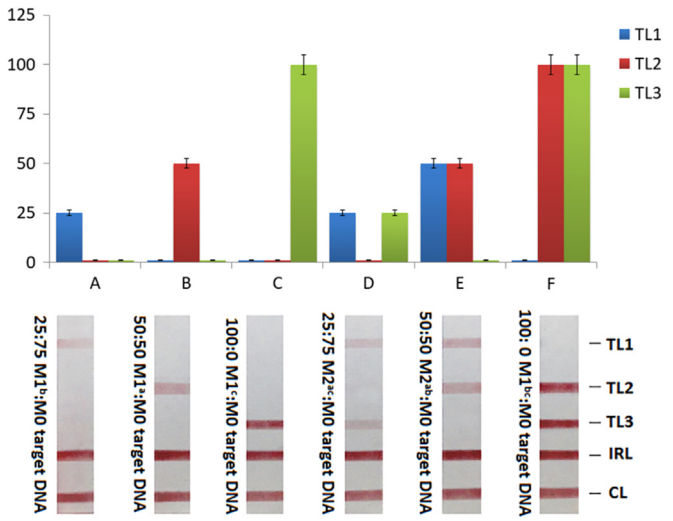

Fig. 3. Typical photograph images (bottom) and corresponding intensities (top) of the LFNABs in the presence of 25:75 $M1^b$:M0 target DNA (A), 50:50 $M1^a$:M0 target DNA (B), 100:0 $M1^c$:M0 target DNA (C), 25:75 $M2^{ac}$:M0 target DNA (D), 50:50 $M2^{ab}$:M0 target DNA (E) and 100: 0 $M1^{bc}$:M0 target DNA (F). The intensities of the bands were recorded by strip reader. (For interpretation of the references to color in this figure, the reader is referred to the web version of this article.)

Quantitative detection was performed by recognizing the peak areas of lines with a portable strip reader. Well-defined peaks occurred, and the peak areas increased with an increase in the M3 concentration. Fig. 2 also shows the relationship between the I (%) (the ratio of peak area of TLs and IRL) and the M% (M%=M3/[M3+M0]). The correlation equation was Δi (%)=0.9634 M%+1.1317 with a correlation coefficient of 0.9906. The moderate linear correlation is a main flaw for the proposed method. The reason is that labeled conjugates show a different behavior in releasing from conjugate pad and linear correlation is weak when labeled conjugate materials are partially released (Saji et al., 2015). There was a linear range over 1–100%, and the limit of detection (LOD) was 1% of M3, which is reasonable and suitable for quantitative work of in-situ measurement according to previous studies (see details in Supporting information).

(2) Discrimination of the methylation level: to implement the detection of DNA methylation with contiguous sites in real samples, it is essential to assess the discrimination of methylation levels against cross-reactivity in biological samples. Six DNA samples, 25:75 $M1^b$:M0 target DNA, 50:50 $M1^a$:M0 target DNA, 100:0 $M1^c$:M0 target DNA, 25:75 $M2^{ac}$:M0 target DNA, 50:50 $M2^{ab}$:M0 target DNA and 100: 0 $M1^{bc}$:M0 target DNA, were used for the PCQ-PCR-LFNAB. The images are shown in Fig. 3. When contiguous multi-methylated sites were detected in one assay, no smear or false positive lines were observed on the strip. As expected, a bright red band was observed on the one of the TLs with M1 DNA (Fig. 3A–C), and a higher concentration of target DNA appears with a darker TL. The selectivity was further demonstrated by detecting M2 DNA, which has two methylated sites (Fig. 3D–F). The intensity difference of the red bands on two of the TLs in the presence of M2 DNA demonstrated the excellent selectivity of the assay. These results demonstrate that the sensing system can distinguish differences in the level of methylated sites.

(3) Reproducibility and stability: the signal reproducibility and analytical stability were two of the most important criteria in evaluating the sensing system. The reproducibility included two parts: device-to-device reproducibility and experimental error reproducibility. The device-to-device reproducibility of the proposed method was evaluated by analyzing one sample for six replicate determinations. Sample solutions containing 0:100 and 50:50 of M3:M0 DNA were used to examine the performance of the LFNAB. As shown in Fig. 4A, similar responses could be obtained against each concentration. The corresponding RSD values of optical responses for 0 and 50% were 1.7% and 2.6%, indicating the excellent device-to-device reproducibility of the measurements.

Experimental error occurred frequently during in situ measurement, such as human error, inhibitory factor existence, DNA extraction efficiency, amplification efficiency, etc. Thus, it is possible for amplification products from the same sample to hold different concentrations under the same operating conditions. The experimental error reproducibility was evaluated by a series of doubling dilutions from the sample solution containing 100:0 of M3:M0 DNA (0.4 μM). As shown in Fig. 4B, although the absolute intensity decreases with the concentration, the relative intensity, namely the proportions of DNA methylation, was approximately equal in samples, indicating the excellent self-correcting capability and experimental error reproducibility of the assay.

The stability was tested by storing the LFNAB at room temperature. Their responses did not change significantly after one month of storage. The intensities of the test bands on the LFNAB for 50:50 of M3:M0 DNA were less than 7% compared to those obtained with the newly prepared LFNAB (data not shown), indicating that the LFNAB has a good stability. These LFNAB approaches are very promising with respect to application for the facile and rapid detection of DNA methylation in real biological samples (see Table S3 in Supporting information).

(4) Application in real samples: to further confirm that PCQ-PCR-LFNAB can be applied for contiguous DNA methylation sites analysis in biological samples, performances were challenged in the complex mice plasma system. In the samples 1–5, genome in mice plasma samples without and with spiked target DNA were extracted using the QIAamp DNA blood mini kit according to the manufacturer's protocol and detected according to the previously

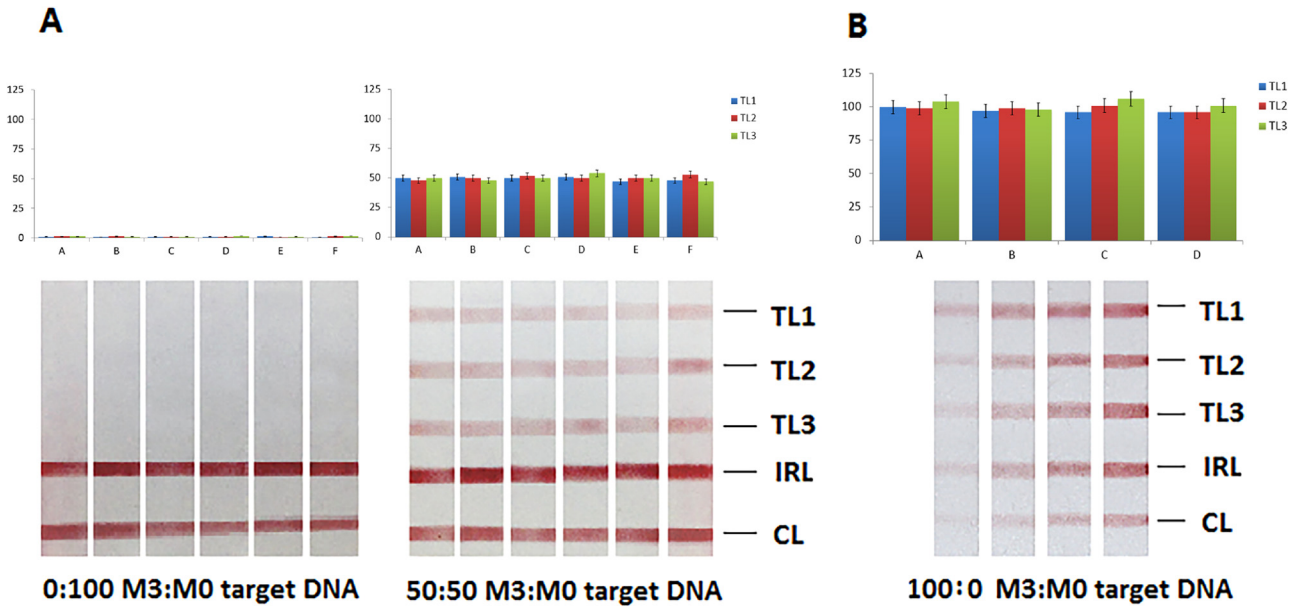

Fig. 4. (A)Typical photograph images (bottom) and corresponding intensities (top) of the LFNABs in the presence of 0:100 M3:M0 target DNA (left) and 50: 50 M3:M0 target DNA (right). The intensities of the bands were recorded by strip reader. (B) Typical photograph images (bottom) and corresponding intensities (top) of the LFNABs in the presence of a series of doubling dilutions from the sample solution containing 100:0 of M3:M0 DNA (0.4 μM) from right to left. The intensities of the bands were recorded by strip reader.

Table 1
Real sample results in the complex blood plasmas system.

Sample	Methylation type	Spiked	Spiked DNA (%)	Detected DNA (%)	Recovery (%)
No. 1	$M1^a$: ($M1^a$+M0)	–	0	0	
		$M1^a$	30	28.3	94.3 ± 0.375
No. 2	$M1^b$: ($M1^b$+M0)	–	0	0	
		$M1^b$	50	48.4	96.8 ± 0.249
No. 3	$M1^c$: ($M1^c$+M0)	–	0	0	
		$M1^c$	70	67.9	97.0 ± 0.318
No. 4	$M3^{abc}$: ($M3^{abc}$+M0)	–	0	0	
		$M3^{abc}$	70	67.4	96.3 ± 0.335
No. 5	$M1^a$+$M1^b$+$M1^c$: ($M1^a$+$M1^b$+$M1^c$ +M0)	–	0	0	
		$M1^a$	30	28.2	94.0 ± 0.331
		$M1^b$	50	47.7	95.4 ± 0.193
		$M1^c$	70	67.0	95.7 ± 0.343

described method. The result for each single sample was summarized in Table 1, which showed that all of the recoveries were greater than 94%. Compared with literatures, the proposed method owns a satisfactory recovery (see Table S2 in Supporting information). Furthermore, the genome of spiked sample 5 was amplified by PCR, cloned into the PGEM-T vector and screened the positive cloning by IPTG-Xgal trial. The plasmid was extracted from positive clones and the inserted target sequences were identified by sequencing in ABI3730XL genetic analyzer (Foster City, Calif) (see details in Supporting information). As a result, there are 110 sequences owning methylated a site, 185 sequences owning methylated b site and 258 sequences owning methylated c site in 384 positive white colonies. The proportion of methylation on site a, b and c are 28.6%, 48.2% and 67.2% respectively, which nearly the same with the results of the proposed method. The above results indicate that the sensing system own satisfactory accuracy and potential applicability for contiguous DNA methylation sites detection in real samples.

4. Conclusions

In summary, we have developed an easy-to-use analysis based on LFNAB for analyzing the PCQ-PCR products in aqueous solutions and biological samples, resulting in accurate quantitative proportion. The proposed assay offers the following distinct advantages over other published methods: (1) identification of the methylation levels of contiguous multi-sites both in aqueous solutions and biological samples; (2) accurate detection due to the proportion competitive system of amplification and the excellent self-correcting capability of the cascade sensing system; (3) high sensitivity from biotin-dUTP to generate multiple biotin attached targets and high selectivity because of a set of specific primers in competition; (4) easy-to-use assay owning self-contained proportion quantitative system are independent of external standard; and (5) only requires inexpensive instrumentation for quantitative. This portable, integrated test model provides a universal platform and shows great promise for in-field and point-of-care diagnosis for other gene's methylation levels by making slight modifications. Furthermore, the biosensor can be extended to detect more sites of DNA methylation with corresponding immune affinity recognitions and be applied to test the reliability of the approach with some real samples from local hospitals and clinics, which will help in disease detection, therapy validation and point of care.

Acknowledgment

This work was supported by the Ministry of Science and Technology of Beijing (XX2014B069) and the National GMO Cultivation Major Project of New Varieties (Grant No. 2014ZX0801202B).

Appendix A. Supplementary material

Supplementary data associated with this article can be found in the online version at http://dx.doi.org/10.1016/j.bios.2016.02.039.

References

Bartlett, J.M.S., Stirling, D., 2003. PCR Protocols. Humana Press, pp. 3–6.
Bi, S., Zhao, T., Luo, B., et al., 2013. Chem. Commun. 49 (61), 6906–6908.
Chen, C., Ridzon, D.A., Broomer, A.J., et al., 2005. Nucleic Acids Res. 33 (20), e179-e179.
Chodavarapu, R.K., Feng, S., Bernatavichute, Y.V., et al., 2010. Nature 466 (7304), 388–392.
Erlich, H.A., Gelfand, D., Sninsky, J., 1991. J. Sci. 252 (5013), 1643–1651.
Fang, Z., Huang, J., Lie, P., et al., 2010. Chem. Commun. 46 (47), 9043–9045.
Fang, Z., Wu, W., Lu, X., et al., 2014. Biosens. Bioelectron. 56, 192–197.
Gao, X., Xu, H., Baloda, M., et al., 2014. Biosens. Bioelectron. 54, 578–584.
Ge, X., Asiri, A.M., Du, D., et al., 2014. TrAC. Trends Anal. Chem. 58, 31–39.
Ge, Y., Wu, B., Qi, X., et al., 2013. PLoS One 8 (8), e69941.
Gu, J., Wen, Y., Zhu, S., et al., 2013. PLoS One 8 (4), e60107.
He, Y., Zeng, K., Zhang, S., et al., 2012. Biosens. Bioelectron. 31 (1), 310–315.
Herman, J.G., Graff, J.R., Myöhänen, S., et al., 1996. Proc. Natl. Acad. Sci. 93 (18), 9821–9826.
Hughes, S., Jones, J.L., 2007. BMC Mol. Biol. 8 (1), 91.
Jha, A.K., Nikbakht, M., Jain, V., et al., 2012. Oncol. Lett. 3 (6), 1331–1335.
Kim, Y.T., Jung, J.H., Choi, Y.K., et al., 2014. Biosens. Bioelectron. 61, 485–490.
Liana, D.D., Raguse, B., Gooding, J.J., et al., 2012. Sensors 12 (9), 11505–11526.
Mao, X., Ma, Y., Zhang, A., et al., 2009. Anal. Chem. 81 (4), 1660–1668.
Nakayama, G., Kodera, Y., Ohashi, N., et al., 2011. Anticancer Res. 31 (5), 1643–1646.
Njiru, Z.K., 2011. Diagn. Microbiol. Infect. Dis. 69 (2), 205–209.
Noguera, P., Posthuma-Trumpie, G.A., Van, T.M., et al., 2011. Anal. Bioanal. Chem. 399 (2), 831–838.
Nolan, T., Bergkvist, A., 2013. PCR Technol.: Curr. Innov., 245.
Ogino, S., Kawasaki, T., Brahmandam, M., et al., 2006. J. Mol. Diagn. 8 (2), 209–217.
Parolo, C., Merkoçi, A., 2013. Chem. Soc. Rev. 42 (2), 450–457.
Porter, J.R., Stains, C.I., Segal, D.J., et al., 2007. Anal. Chem. 79 (17), 6702–6708.
Razin, A., Riggs, A.D., 1980. Science 210 (4470), 604–610.
Saji, M., Kawde, A.N., Daud, M., 2015. J. Saudi Chem. Soc. 19 (6), 689–705.
Shelton, D.N., Litterst, C., Regan, J.F., et al., 2014. Cancer Res. 74 (19 Suppl.) 2301 – 2301.
Suzuki, M., Yamada, T., Kihara-Negishi, F., et al., 2006. Oncogene 25 (17), 2477–2488.
Torres-Chavolla, E., Alocilja, E.C., 2011. Biosens. Bioelectron. 26 (11), 4614–4618.
Tost, J., Gut, I.G., 2007. Nat. Protoc. 2 (9), 2265–2275.
Tsou, J.A., Hagen, J.A., Carpenter, C.L., et al., 2002. Oncogene 21 (35), 5450–5461.
Wang, W.S., Pan, Y.J., Zhao, X.Q., et al., 2010. J. Exp. Bot., erq391
Wang, X., Zhu, Y.B., Cui, H.P., et al., 2014. Tumor Biol. 35 (9), 9035–9043.
Watson, J.D., 2012. Springer Science & Business Media, pp. 3–5.
Zachar, V., Thomas, R.A., Goustin, A.S., 1993. Nucleic Acids Res. 21 (8), 2017.
Zerilli, F., Bonanno, C., Shehi, E., et al., 2010. Clin. Chem. 56 (8), 1287–1296.
Zhou, L., Palais, R.A., Paxton, C.N., et al., 2015. Clin. Chem. 61 (5), 724–733.